



Method for polychlorinated biphenyls removal from mussels and its photocatalytic dechlorination

Renugambaal Nadarajan, Wan Azelee Wan Abu Bakar*, Rusmidah Ali, Razali Ismail

Department of Chemistry, Faculty of Science, Universiti Teknologi Malaysia, 81310 UTM, Johor Bahru, Johor, Malaysia



ARTICLE INFO

Article history:

Received 16 March 2017

Received in revised form 14 June 2017

Accepted 21 June 2017

Available online 23 June 2017

Keywords:

Polychlorinated biphenyl

Polyethylene glycol

Mussel

Photocatalysis

Trimetallic oxide

ABSTRACT

A simple method has been proposed for the removal and degradation of polychlorinated biphenyls (PCBs) from catches using low cost and environmental friendly way. The removal of PCBs from lipid layer to aqueous layer was done by utilizing polyethylene glycol (PEG) as phase transfer agent and photocatalysis technology for its degradation. Experimental involving various types of PEG and concentrations were performed to obtain the highest percentage of removal. The highest total amount of PCBs removal was attained using PEG 400 with concentration of 0.2 M. In order to determine the suitable photocatalyst to use for the degradation study, the physicochemical properties of $\text{WO}_3/\text{SnO}_2/\text{TiO}_2$ prepared from mechanical mixed and sol-immobilization were compared. In situ and ex situ techniques were explored to determine its influence on removal and degradation of PCBs. Substantial degradation of removed PCBs in ex situ method was achieved in the presence of heterostructured $\text{WO}_3/\text{SnO}_2/\text{TiO}_2$ photocatalyst prepared by mechanical mixing under visible light. Meanwhile significant total amount of PCBs reduction in mussels was observed under in situ method (with PEG 400, 0.2 M and photocatalyst) compared to control run. Thus, this study displayed conformity of the method with high degradation.

© 2017 Elsevier B.V. All rights reserved.

1. Introduction

Studies have been conducted worldwide monitoring the level of polychlorinated biphenyls (PCBs) in marine water, sediments, fish, mussels and also in human (from breast milk and serum) [1–10]. PCB with different number of chlorine atoms attached to biphenyl rings are highly lipophilic which bioaccumulate in fatty tissue of aquatic lives and subsequently lead into the food chain. The concentration of PCBs varies according to countries and sampling sites. In Southeast Asia, concentration of PCBs detected in sediments was much higher than those found in mussels but are relatively low in fish [1,11–15]. Conversely higher PCBs level was reported in fish samples at several countries in United States and Europe [16–19]. Despite of its low concentration, PCBs has detrimental effect on human health which includes reproductive and developmental effects, neurological and behaviour effects, dermal toxicity and carcinogenic effect [20]. The main cause of PCBs detection in human is through the daily intake especially fish and seafood [20,21]. Even though stringent controls have been imposed on these products to minimize the impact on human

health [22], yet the occurrence of PCBs in aquatic lives are still being reported.

This leads to numerous studies to reduce the bioaccumulation of PCBs in aquatic lives. Since aquatic sediment act as a sink for hydrophobic organic pollutants [23], the research works were concentrated on PCBs removal from sediments. One of the most investigated areas was in situ treatment using activated carbon as being effective and low cost compared to the conventional method of dredging and capping [24–29]. Various other techniques that have been explored include bioremediation [30], dechlorination [31], adsorption and biodegradation [32]. However, remediation of contaminated sediments remains a technological challenge pertaining to the large area coverage that might incur high cost and longer treatment time. It has been reported that fish and seafood is one of the highest daily intake [33]. To the best of our knowledge, no research work has been done on PCBs removal from the aquatic lives or sea catches. Therefore, development of new techniques offering greater flexibility in reducing the amount of PCBs in sea catches prior to consumption is highly desirable.

Recently, Azlee et al. [34] has conducted research work on the removal of heavy metals from mussels via catalytic oxidation using sodium acetate as chelating agent. This has inspired us to explore on the removal of PCBs from catches using phase transfer agent such as polyethylene glycol. Polyethylene glycol (PEG) is a bifunc-

* Corresponding author.

E-mail address: wazelee@kimia.fs.utm.my (W.A.W.A. Bakar).

tional amphiphilic polymer with reactive OH groups on both ends and has been widely used in biological and food chemistry because of the advantages of high water solubility, nontoxicity, low cost, facile biodegradation, and environmental friendliness [35]. In earlier years, PEG has been used to transfer PCBs from transformer oils or dielectric fluids into a non-polar solvent using solvent extraction method prior to dehalogenation using NaPEG [36]. PEG was also effectively used as phase transfer agent together with potassium hydroxide (PEG/KOH) for removing and decomposition of PCBs in non-polar fluids or oils under thermal treatment [37–39]. In addition, enhanced dechlorination of tetrachloroethylene by zerovalent silicon with the addition of PEG 400 has also been reported [40].

Meanwhile photodegradation method has been known as feasible remediation for PCBs. Effective photodechlorination of PCBs at longer wavelength and possible use of visible light or sunlight has been a topic of considerable interest. Recently, surface modifications to the electronic structure of titanium dioxide in order to shift the absorption into the visible range and to reduce the charge recombination are under intense study in the photocatalysis field. The most common type of alteration involves structural defects with exposed facets and surface defects, which could be achieved by modifying the preparation method and calcination temperature. On this basis, the most studied metal oxides with exposed facets and surface defects are TiO_2 , WO_3 , SnO_2 , and ZnO which has contributed to high catalytic activity by improved charge carrier separation [41]. TiO_2 coupled SnO_2 or WO_3 [42,43] with the presence of surface defects has gained additional importance due to enhanced activity under visible light with efficient charge separation. The improved charge separation is not only the main criteria for higher photocatalytic activity but the photocatalyst should also have good adsorption ability of pollutants on the surface of the photocatalyst. High surface acidity of WO_3/TiO_2 photocatalyst has been reported to improve adsorption of hydroxyl group as well as organic reactants on its surface which facilitate the enhancement of photocatalytic activity [44]. From our earlier study, rutile TiO_2 and $\text{WO}_3/\text{SnO}_2/\text{TiO}_2$ photocatalyst has exhibited high catalytic activity in the degradation of 1,2-dichlorobenzene which was used as model PCB [45,46]. The as-prepared photocatalyst with the presence of Ti^{3+} in rutile TiO_2 and oxygen vacancies has demonstrated effective charge transfer which resulted in enhancement of activity under visible light compared to UV light.

Therefore, the aim of this study was to explore removal of PCBs from unshelled catches by adding food grade PEG and then degrade it by irradiation using light. PEG is used as phase transfer agent to remove PCBs from unshelled catches into aqueous. The removed toxic PCBs in aqueous could then be degraded to lower chlorinated or non-toxic compounds in the presence of visible light active photocatalyst and day use fluorescent lamp as visible light source. The photocatalyst should be immobilized on support material that does not leach to ensure its safe usage.

In this paper, the physicochemical properties of as-prepared $\text{WO}_3/\text{SnO}_2/\text{TiO}_2$ by mechanical mixing and sol-immobilized were compared and the potential photocatalyst was used to evaluate its effectiveness in degradation of PCBs. Since the occurrence of PCBs in mussels has been widely reported, green mussels (*Perna viridis*) were used as the model. Two different techniques had been investigated. Firstly, a known concentration of removed PCBs in aqueous was treated to justify the per cent degradation (referred as ex situ). In the second technique, in situ removal of PCBs from green mussels with spontaneous PCBs degradation in the presence of PEG and photocatalyst were investigated. In both experiment, immobilized photocatalyst on PVC film was used and has insignificant leaching as shown in our previous study [45]. Therefore this technique is safe and cheap. In view of that, to the best of our knowledge, this study is the first attempt to rationalize the feasibility of PCBs removal from catches as green mussels using cost effective technique.

2. Experimental

2.1. Materials

Polyethylene glycol (PEG) 400, 600 and 2000 were obtained from Merck. Standard solution of PCB 15, 28, 52, 138 and 153 (10 ppm in isoctane) were purchased from Dr. Ehrenstorfer, GmbH. For catalyst preparation, titanium tetraisopropoxide (TTIP) and tungstic acid (H_2WO_4) were purchased from Sigma Aldrich, tin (IV) chloride ($\text{SnCl}_4 \cdot 5\text{H}_2\text{O}$) from Bendoson Lab, diethanolamine (DEA), tetrahydrofuran (THF) and polyvinyl chloride (PVC) from Merck while ethanol (EtOH) and hydrogen peroxide 30% solution were obtained from Qrec. All chemicals were used as received. Dichloromethane, hexane and isoctane solvent plus anhydrous sodium sulphate were procured from Merck.

2.2. Photocatalyst preparation

The detailed preparation method has been described elsewhere [45]. In brief, TiO_2 was prepared using 12 g of TTIP which was added into mixture of ethanol:PEG 2000 (1:1.43) and DEA (6.15 g). 1.60 mL of distilled water was added at the end. To prepare WO_3 , tungstic acid (5.4 g) was completely dissolved in H_2O_2 (100 mL), aged for one day and then added with 1.35 g of PEG 2000. $\text{SnCl}_4 \cdot 5\text{H}_2\text{O}$ (8.76 g) were dissolved in mixture of EtOH: H_2O (1:1) to obtain SnO_2 sol solution.

To prepare the mechanical mixed sample, all the sol solutions were then autoclaved at 170 °C for 5 h and the obtained products were dried in oven. The dried powder was then calcined at individual optimum temperature as following: TiO_2 at 950 °C, WO_3 and SnO_2 at 850 °C for 5 h. The attained products were mixed using shaker and manually ground in the ratio of 80:10:10, which was the best ratio as disclosed in previous publication [46] and labelled as WST-M. For the sol-immobilized photocatalyst preparation, WO_3 and SnO_2 sol solution were mixed with TiO_2 powder calcined at 950 °C. The mixture was then autoclaved at 170 °C for 5 h. The obtained product were dried in oven for a day and calcined at 900 °C for 5 h. The sample prepared using sol-immobilized method is referred as WST-I. The suitable powder photocatalyst (0.25 g) was then spread on top of semi-solid layer of PVC film prepared by dissolving 1 g of PVC in 25 mL THF solution and left for 10 min in a petri dish to form thin film.

2.3. Catalyst characterization

The XRD powder diffraction pattern was obtained from X-ray diffractometer BrukerAXS D5000 with Cu K α radiation ($\lambda = 1.5406 \text{ \AA}$, 40 kV, 30 mA, 0.050°, 1 s). UV-vis near infrared spectra was recorded using Shimadzu UV3101PC spectrophotometer. The surface morphologies were acquired from field emission scanning electron microscopy (FESEM, SU8020, Hitachi) and transmission electron microscopy (TEM, JEOL-TEM 2100). Surface roughness was measured using atomic force microscopy (AFM, Seiko SP13800N) with dynamic force mode sample holder and NanoNavi analysis software. NH₃ temperature-programmed desorption (NH₃-TPD) was performed on Micromeritics Autochem 2920 conditioned as following: sample cleaning using He flow (10 cm³/min, 200 °C, 2 h), cooling to 45 °C followed by sample heating under NH₃(10%):He(90%) at 45 °C (1 h) and increased to 1000 °C (10 °C/min). The specific surface area (BET) was obtained from N₂ adsorption/desorption analysis conducted using Micromeritics ASAP 2010. Meanwhile Malvern Zetasizer Nano ZSP was used to measure the zeta potential to predict the surface charge. The adsorption of organic molecule on catalyst surface was performed on Thermo-Nicolet FTIR Spectrometer equipped with multireflection ATR mounted with germanium crystal.

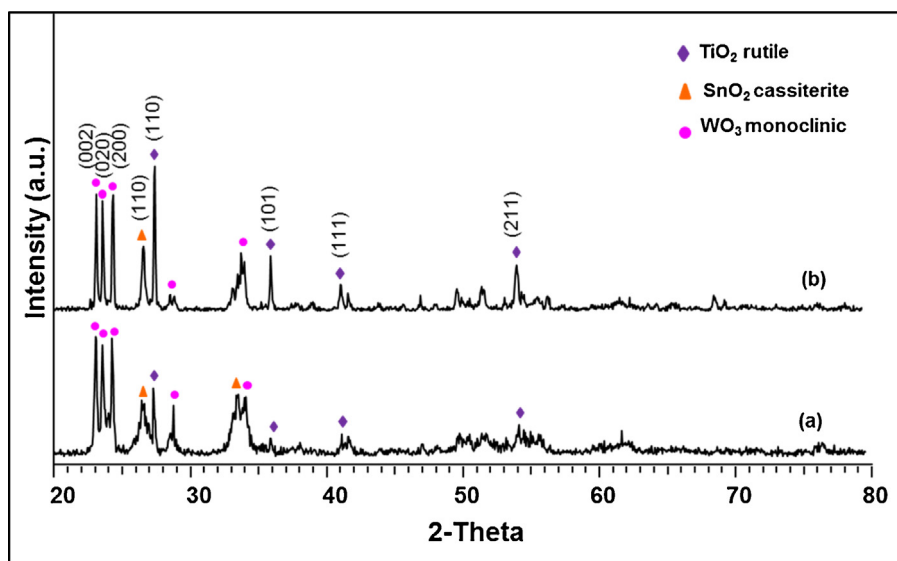


Fig. 1. XRD diffractogram pattern obtained for (a) WST-I and (b) WST-M.

2.4. Removal of PCBs from mussels into aqueous layer

The effect of different molecular weights of PEG and its concentration on the removal of PCB was investigated using PEG 400, PEG 600 and PEG 2000 with concentration ranging from 0.05 M to 0.3 M. The green mussels were collected randomly from sampling site at Sungai Melayu located at Johor Strait, Malaysia as shown in Fig. S1 and cleaned. The removal study was conducted by dipping three live mussels (with length of approximately 5–7 cm) in 250 mL of distilled water containing different type of PEG and concentration. The aqueous solution was continuously stirred and samples were collected at 2, 4, 6 and 8 h. A control test without the presence of PEG was also performed. The collected aqueous samples containing PCB and undissolved organic matters were isolated using liquid–liquid extraction method. Isooctane solvent (2 mL × 3) was utilized to extract the PCB from aqueous and then dried with 1 g of anhydrous sodium sulphate. The extracts were then concentrated to 1 mL using rotary evaporator followed by drying under nitrogen gas flow for about 2 min. The type and concentration of PCB removed from mussels was determined in relation to standard PCB calibration by GC-ECD.

2.5. Extraction of PCBs from mussels

The mussels flesh weighed about 13–16 g were homogenised with anhydrous sodium sulphate using a mortar and pestle. Homogenates of the mussels flesh were soxhlet extracted for 22 h using 200 mL of dichloromethane:hexane (1:1) followed by one day aging. The extract was then filtered with filter paper containing 5 g of anhydrous sodium sulphate to remove lipid precipitation and traces of water prior to purification using Supelco LC-18 SPE. The cartridge was topped with activated silica gel (1 g):anhydrous sodium sulphate (1 g) and conditioned with 5 mL of methanol followed by 5 mL dichloromethane:hexane (1:1) under vacuum suction. Then, the extracted aliquots were loaded at a flow rate of approximately 1 mL/min. Elution was performed with 5 mL of dichloromethane:hexane (1:1). The eluates obtained were concentrated by rotary evaporation followed by drying under nitrogen flow. The concentration of PCBs in mussels after the removal process was determined by GC-ECD. The initial concentration of PCBs in mussel was based on the sum of PCBs identified in aqueous and mussels.

2.6. Degradation of PCB in aqueous

In this experiment, the PCBs removal from live green mussels was foremost conducted by using the best PEG and concentration. After 8 h of exposure, the mussels were removed and the aqueous solution was used for the photocatalytic degradation study. The photodegradation reaction was conducted in a closed reactor using $\text{WO}_3/\text{SnO}_2/\text{TiO}_2$ photocatalyst immobilized on PVC film and irradiated with compact fluorescent light ($\lambda > 400 \text{ nm}$, 36 W) for 6 h. The aqueous samples were collected every hour and PCBs were extracted according to steps described in Section 2.4 prior to analysis using GC-ECD.

2.7. Gas chromatography with electron capture detector (GC-ECD)

GC-ECD analyses were done on a Perkin-Elmer Clarus 680 gas chromatograph equipped with electron capture detector (ECD) utilizing HP-5MS (5%-phenyl-methylpolysiloxane) capillary column (length:30 m, internal diameter:0.25 mm and film thickness:0.25 μm). Helium was used as the carrier gas and N_2 as makeup gas. The injector port was set at 250 °C. The chromatographic conditions were: column temperature program set at 200 °C (2 min), increased to 230 °C (7 °C/min) and 290 °C (2 min, 12 °C/min); injector temperature was set at 300 °C with split ratio of 50:1; ECD temperature was set at 350 °C. Prior to the analysis, the retention time for each PCB (PCB 15, 28, 52, 138 and 153) was determined by running the mixture of PCB standards followed by calibration for each PCB (Figs. S2 and S3).

3. Results and discussion

3.1. Catalyst characterization

The composition of the prepared photocatalyst was confirmed from the obtained XRD diffractogram (Fig. 1). The presence of three sharp peaks at lower range $2\theta = 23.08^\circ$, 23.55° , 24.03° with hkl (002), (020) and (200) reflects WO_3 in monoclinic form in accordance to JCPDS 072-0677. Peak at $2\theta = 26.59^\circ$ reflects the existence of (110) plane of SnO_2 rutile in cassiterite (JCPDS 072-1147). Meanwhile the major peaks at $2\theta = 27.45^\circ$, 36.09° and 41.25° belongs to TiO_2 rutile (110), (101) and (111) plane respectively in accordance

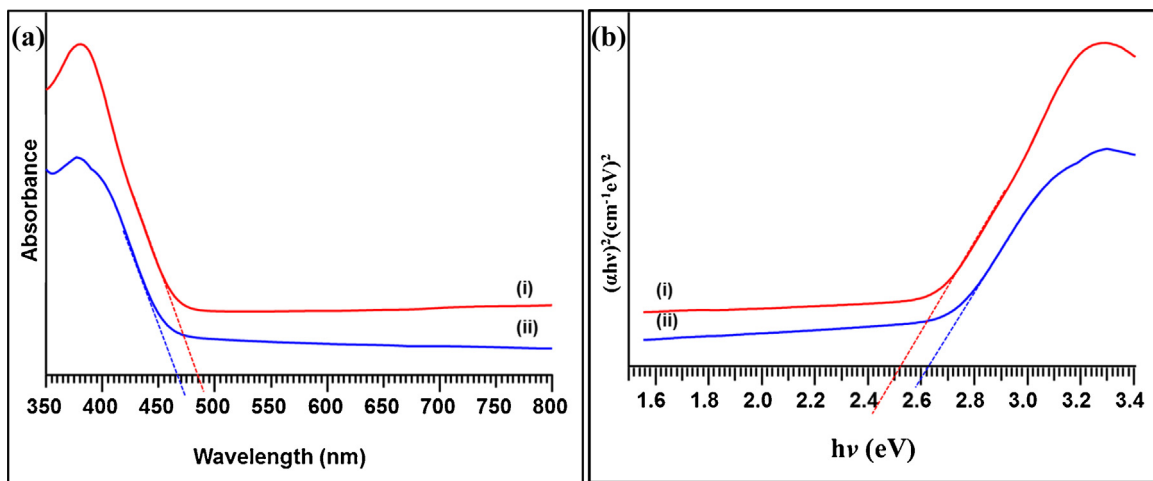


Fig. 2. (a) Absorption spectra and (b) band gap value for (i) WST-M and WST-I.

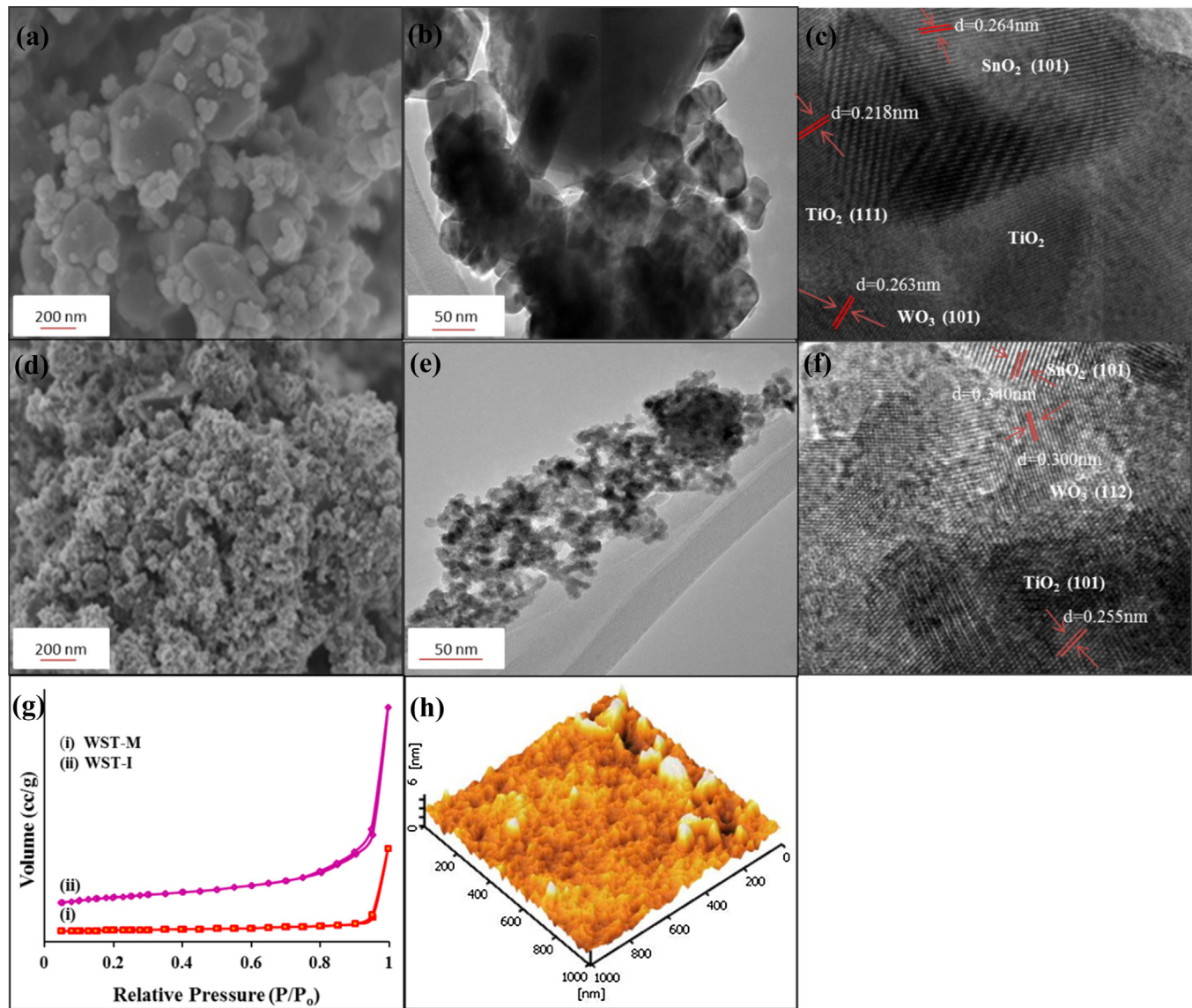


Fig. 3. FESEM, TEM and HRTEM image for WST-M (a–c) and WST-I (d–f) photocatalyst, (g) BET surface area and (h) AFM image showing surface roughness of WST-M photocatalyst after immobilized on PVC film.

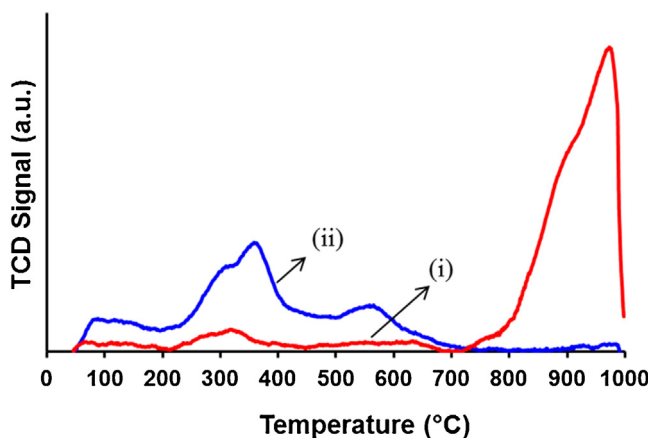


Fig. 4. NH_3 -TPD showing TCD signal against desorption temperature profile for (i) WST-M and (ii) WST-I photocatalyst.

to JCPDS 89–4202. High intensity of TiO_2 peaks was observed for WST-M sample that displays high crystallinity. On the other hand, WST-I sample shows amorphous pattern with suppressed TiO_2 . No other impurity peaks indicating the purity of the sample as well as non-occurrence of metal oxide doping.

Based on data obtained from UV-vis near infrared analysis, the photon light absorption and band gap of the photocatalyst was determined. As illustrated in Fig. 2a, the absorption edge was for WST-M and WST-I are at 485 nm and 465 nm respectively. This result also corresponds to its low band gap value of 2.52 eV for WST-M and 2.62 eV for WST-I which indicates its potential use under visible light region.

Morphological structure of the photocatalyst acquired from FESEM and TEM was shown in Fig. 3(a–f). The images obtained for WST-M sample (Fig. 3a and b) showed mixture of large and small particles has particle size in the range of 18–470 nm that displays low surface area ($4.3 \text{ m}^2 \text{ g}^{-1}$). In addition, the nanosteped structured particles with slight faceting showed close contacts between the metal oxides. This was also favoured by HRTEM image (Fig. 3c) that displayed the interface between the metal oxides. According to Wang et al. [47], such structures implied the formation of heterojunction between the metal oxides which is essential for charge transfer enhancement and thus promote the activity. On the other hand, from Fig. 3(d–f) it could be noted that the TiO_2 particle with the size of 42.2 nm (Fig. 3e, dark spot) was almost covered by agglomeration of WO_3 and SnO_2 small particles (7–12 nm). Besides, TEM image clearly shows the absence of exposed particles with nanosteped edges which were prominent in sample prepared by mechanical mixing. The suppressed TiO_2 particles were also supported by amorphous XRD diffractogram pattern (Fig. 1(ii)) and wide scan XPS (Fig. S4). This might cause inefficient absorption of light by TiO_2 and thus reduced charge transfer efficiency that might lead to decline in photocatalytic activity despite of its large surface area ($24.7 \text{ m}^2 \text{ g}^{-1}$) as depicted in Fig. 3g. The exposed protruding surface of photocatalyst prepared by mechanical mixing after immobilization on PVC thin film was further examined using AFM. Fig. 3h portrays three dimensional image of the photocatalyst surface immobilized on PVC film. The high root-mean-square roughness value ($R_{\text{rms}} = 7.293 \text{ nm}$) demonstrated good surface roughness which plays a crucial role for the enhancement of photocatalytic activity.

The NH_3 -TPD was performed to investigate the surface acid amount and strength of the catalysts. Fig. 4 displays NH_3 -TPD profile of the catalyst prepared by different methods as a function of desorption temperature. As shown in Fig. 4, the NH_3 -TPD results showed that the preparation method has a significant effect on

the acidic properties of the catalysts. All the NH_3 desorption profiles of the samples could be categorised to two distinct desorption processes: the NH_3 desorption peaks centered at low temperature (lower than 400 °C) assigned to weak acid sites, and the other NH_3 desorption peaks centered at high temperature (higher than 600 °C) originating from strong acid sites [48,49]. It could be inferred that the desorption peak at low temperature is assigned to NH_3^{+} ions bound to the Bronsted acid sites, while the desorption peak at high temperature is associated with NH_3 molecular originating from the Lewis acid sites. [48,50] It should be pointed out that the area of desorption peak is directly proportional to the acid amount and the peak position is correlated with the acid strength. However the position of peaks, its shape, size and surface acidity is greatly affected by nanoparticle surface coordination environment [51] which could be the reason for the differences in shape of NH_3 -TPD spectra between both samples. From Fig. 4, compared with WST-I, the WST-M have less Bronsted acid sites but provides more Lewis acid sites. Besides, the strength of Lewis acid on the WST-M is stronger. According to report by Nakajoh et al. [52], solid acid containing Lewis acid and Bronsted acid, with acidity in the range of 0.1–1.0 mmol/g and acid strength less than 4.0 is desired for good adsorption of aromatic halogenated compound as PCB. Thus, mechanical mixed photocatalyst with high acidity and acid strength of 0.53 mmol/g and 3.85% respectively, could be associated with the strongest interaction/adsorption between metal oxides and PCBs.

The zeta potential value for samples suspended in distilled water in low concentration and at neutral pH was measured which could be ascribed to the surface properties of different samples. The zeta potential of WST-M and WST-I sample was found to be -45.9 mV and -56 mV respectively indicating negatively charged surface. Zeta potential of WST-I is more negative than that of the WST-M, indicating favourable adsorption of PCB molecule on WST-M at neutral pH.

Therefore based on the physicochemical properties of $\text{WO}_3/\text{SnO}_2/\text{TiO}_2$ photocatalyst prepared by mechanical mixing and sol-immobilization, it could be inferred that WST-M with better structure and stronger acidity would enhance the adsorption of PCBs onto catalyst and thus exhibit better photocatalytic activity. As such, WST-M photocatalyst were used to study the photocatalytic degradation of PCBs from mussels.

3.2. Removal of PCBs from mussels using PEG

As a first step to determine the possibility of PCBs removal from mussels into aqueous layer, a blank test was conducted in the absence of polyethylene glycol (PEG). The aqueous with untreated mussels did not show any presence of PCBs as displayed by the GC-ECD chromatogram (Fig. S5). The experiment was then extended to study the influence of several types of PEG and different dosage on excretion of PCBs from mussels into aqueous layer. Several analyses conducted to determine the initial PCBs concentration in mussels, showed that the concentration of each PCBs congeners and total PCBs in mussels varies even in a same batch of sample. Therefore all the results presented are based on average of three experimental run.

The effect of PEG 400, 600, 2000 using concentration of 0.05–0.02 M is displayed in Fig. 5 while result with 0.03 M PEG is shown in Fig. S6. Based on Fig. 5(a–c), the utilization of PEG 400 clearly signifies removal of PCBs from mussels at high concentration. The percentage of PCB 15, PCB 52 and PCB 153 detected in aqueous improved as the concentration of PEG 400 increased from 0.05 to 0.2 M and accordingly reflects the reduction of these PCBs in the mussel.

It could be noted that the removal of PCB 15 was tremendously good due to its symmetrical structure with two chlorine atoms

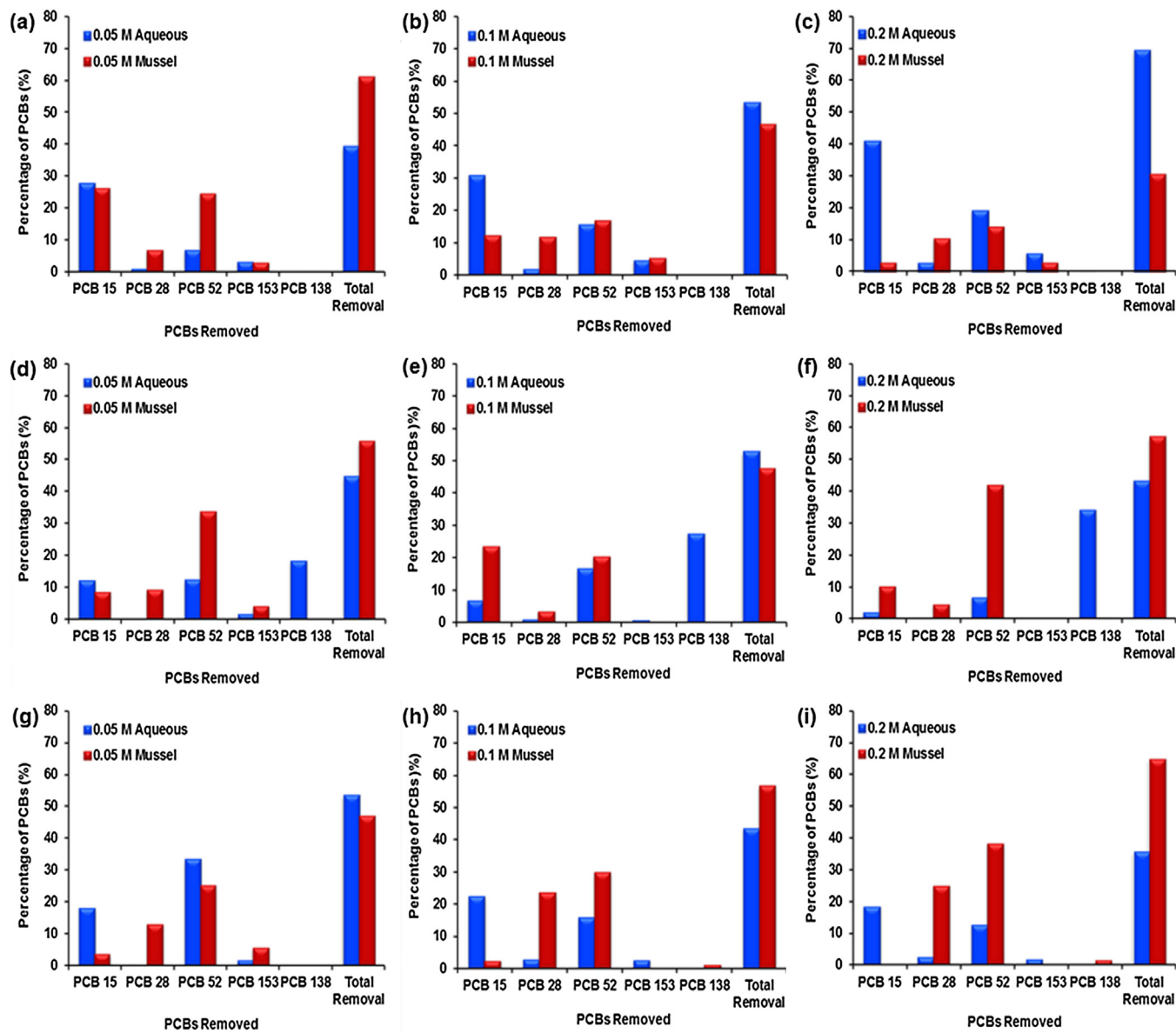


Fig. 5. Percentage of PCBs in aqueous and mussels after the removal using PEG 400 (a–c), PEG 600 (d–f) and PEG 2000 (g–i) at concentration of 0.05 M, 0.1 M and 0.2 M.

and its solubility in water. Similarly the removal of PCB 52 with four chlorine atoms on symmetrical structure also increased along with the concentration of PEG 400. PCB 138 and PCB 153 are the higher chlorinated PCB in this study, with six chlorine atoms on the biphenyl structure at different positions. From the result, the excretion of PCB 138 and PCB 153 was greater using PEG 400 at concentration of 0.2 M. However the removal percentage of PCB 138 in aqueous is not observable in Fig. 5(c) due to its low content in mussel (0.20–0.54%). The dissimilarity in the removal trend could be due to the difference in PCBs concentration in the mussels itself. Therefore total removal of PCBs was used to determine the best concentration. From the analytical result, greater PCBs excretion from mussels into aqueous layer was observed with PEG 400 (0.2 M) which resulted in a total removal of 69.36%.

On the other hand, large amount of PCBs were removed at concentration of 0.1 M when exposed with PEG 600 but subsequently declined with the increase in concentration (Fig. 5(d–f)). The total PCBs removed at 0.1 M concentration (52.67%) however was much lower than the result obtained by using 0.2 M of PEG 400. Substantially great excretion of higher chlorinated PCB 138 was observed

using PEG 600 which gives a hint on its selectivity pattern. The reason of this trend could be attributed to the different repartition coefficient of PCBs between the lipid phase and the glycol. The increase of PEG molecular weight can cause an increased solubility of PCB species in PEG, thus favouring the subtraction of higher chlorinated PCBs [53]. Similarly using PEG 2000 (Fig. 5(g–i)), removal of PCB 15 and PCB 52 was greater especially at concentration of 0.05 M. Nevertheless, the maximum total amount of PCBs in aqueous observed at concentration of 0.05 M (53.36%) was still lower than those achieved employing PEG 400 (0.2 M). From Fig. 5, it could be noted that PCB 28 with three chlorine atoms was hardly removed probably due to the electronic charge distribution on biphenyl ring. It's predicted that lipid bulk phase containing the higher electronic charge phenyl ring may hinder interaction between PCB and PEG.

Based on our experimental data, the total PCBs removal decreased with increasing molecular weight of PEG. This is actually in contrast with the findings of Brunelle and Singleton [54] who claimed that higher molecular weight PEG improves the reaction rate of phase-transfer reaction. On the other hand, Xiao et al. [55] reported that increase of PEG molecular weight would induce steric

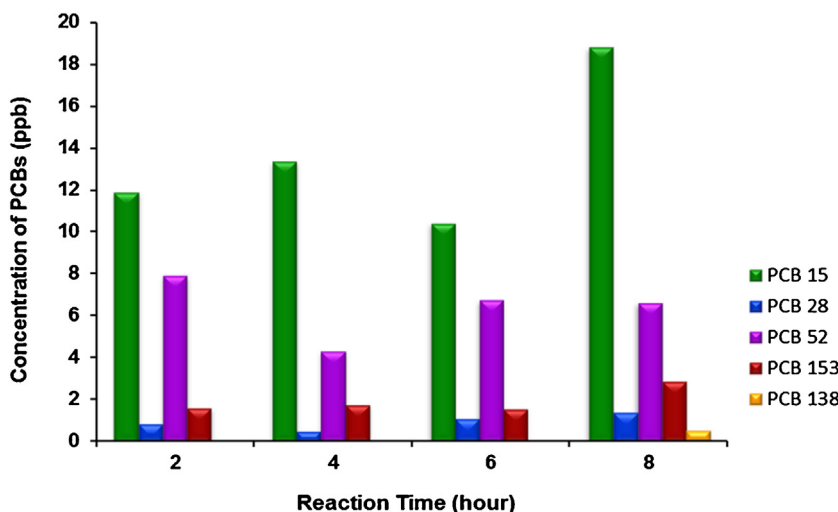


Fig. 6. Concentration of PCBs in aqueous after removal from mussels with 0.2 M of PEG 400.

effect of the substituent group that may result in the reduction of removal rate especially for higher chlorinated PCBs excretion. Besides, PEG with larger molecular weight has higher viscosity and melting point which may also affect the rate for PCBs transferring into reaction media, thus reducing the removal efficiency. Therefore, these results indicate that the addition of PEG 400 with 0.2 M concentration is essential for higher amount of PCBs removal from mussels.

The selectivity and removal trend of PCBs during the sampling for every 2 h was further evaluated upon the addition of PEG 400 (0.2 M). As depicted in Fig. 6, the removal pattern is inconsistent for all the PCBs which could be due to the respiration process of live mussels. Nevertheless higher concentration of all the PCBs was detected after 8 h of exposure with PEG 400. It could be noted that large amount of PCB 15 and PCB 52 were removed. The ease in excretion of PCB 15 and PCB 52 into aqueous layer could be ascribed to their symmetrical structured biphenyl that does not hinder its binding with hydroxyl group in PEG.

3.3. Degradation of PCBs in aqueous after removal from mussels

The best type of PEG and concentration that could excrete larger amount of PCBs from mussel, into aqueous layer was then applied to explore the degradation of PCBs. This study involves two steps which is the removal of PCBs from mussels using PEG 400 (0.2 M) followed by photocatalytic degradation of the removed PCBs in aqueous. The photolysis of PEG 400 (0.2 M) was foremost investigated as shown in Fig. S7. The absence of peaks in the GC chromatogram reflects the stability of PEG 400 under visible light.

After 8 h of removal process, the concentration of PCBs in aqueous sample was determined and referred as initial concentration. PCBs absorb radiation in the mid-UV spectral range and thus in this study direct photolysis was negligible [56]. Meanwhile the adsorption of PCB in dark as presented in inset of Fig. 7 and the presence of C–Cl at wavelength 1017 cm^{-1} in FTIR spectra (Fig. S8) demonstrated good adsorption of PCBs onto the photocatalyst in neutral solution. Subsequent photocatalytic reaction exhibited high dechlorination (83.7%) of the total PCBs. Fig. 7 displayed the initial concentration of PCBs in aqueous as well as at different interval during the reaction. The GC-ECD chromatogram showing dechlorination of PCBs was presented in Fig. S9.

The result showed that more than half of the total PCBs (64.5%) was degraded at the initial 1 h of reaction and the decomposition rate decreased along with reaction time. It was presumed that

the hydroxyl radical generated during the photocatalysis process attacked the C–Cl bonding points of PCBs in the first stage of degradation pathways. Mullin et al. [57] reported that the numbers and locations of chlorine atom on PCB congeners were the most important criteria for the evaluation of PCBs degradation. Besides, the ease of chlorine atom elimination was reported to follow the order of ortho- > meta- > para substituted chlorine [58].

In this experiment, trichlorobiphenyl PCB 28 was degraded much faster than dichlorobiphenyl PCB 15 which might be due to a high concentration of PCB 28. From the previous studies, it is known that the degradation of PCBs occurs by losing one chlorine atom at a time, thus increasing the concentration of less chlorinated species. This behaviour is markedly evident in the next second hour of sampling with the increase of PCB 15 following the reduction of PCB 28. The subsequent samplings also indicated higher amount of PCB 15. This can be rationalized considering that the activity of the reaction, although low, was aimed at the degradation of high chlorinated biphenyls (tri-, tetra- and hexa-chlorobiphenyls) which gave lower chlorinated species [53]. Besides, PCB 15 being a non-ortho PCB has been reported to exhibit slow degradation rate [59].

It was also notable that the concentration of PCB 52 after 1 h of irradiation was almost similar to the initial concentration. This could be correlated to the degradation of PCB 153 to lower chlorinated biphenyls. PCB 153 is a symmetrical biphenyl with chlorine substituents in the ortho, meta, and para positions of both rings was proposed to be reduced to PCB 101 and then PCB 52 [59]. Another reason might be explained by the specific molecular structure of congener 52. Even though PCB 52 is a symmetrical biphenyl with chlorine substituents in the ortho and meta positions, the bond lengths of carbons with *ortho*-chlorines and *meta*-chlorines is 1.746 and 1.746 respectively, which is identical thereby causing steric hindrance [60]. The subsequent degradation of PCB 52 in low concentration however could not be justified as the expected degraded intermediates would be trichlorobiphenyl (PCB 18) and bichlorophenyl PCB 11 [61].

On the other hand, the degradation of hexachlorobiphenyl PCB 138 with ortho, meta and para located chlorine atoms was much slower than hexachlorobiphenyl PCB 153. This could be related to research work by Lin et al. [58] which revealed that PCB 138 exposed to UV light (254 nm) had more significant effect on the decomposition compared to when visible light in the wavelength of 380–780 nm was used. Eventually, substantial degradation was observed with 83.7% reduction of total PCBs after 6 h of reaction. The overall photocatalytic degradation was enhanced in the presence

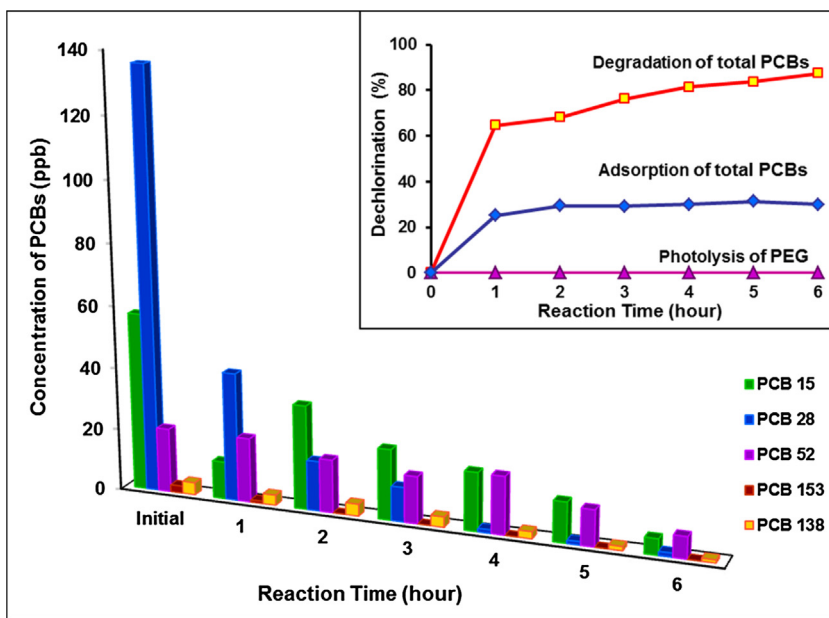


Fig. 7. Concentration of PCBs in aqueous after the removal process from mussel (labelled as initial) and upon degradation using immobilized $\text{WO}_3/\text{SnO}_2/\text{TiO}_2$ photocatalyst under visible light for 6 h. Inset graph showing the photolysis of PEG 400 (0.2 M), adsorption and dechlorination of total PCBs.

of WST-M photocatalyst under visible light irradiation. Eventually, the experimental data on PCBs removal followed by the photocatalytic degradation confirms the feasibility of the method for a real time application. Further study on using mixture of different type PEG ratios for the removal of lower and higher chlorinated PCBs as well as the by-products determination is needed for better understanding.

3.4. In-situ PCBs removal from mussels and its degradation in aqueous

The possibility of in-situ PCBs removal from mussel and degradation was also explored in relative to the above discussed technique (Section 3.3). In this study, in situ removal of PCBs and degradation was evaluated in the presence of PEG, immobilized WST-M photocatalyst and visible light. As the initial concentration of PCBs in mussels are not known, a control test using the same batch and size of mussels but without the photocatalyst was conducted as comparison and presented in Fig. 8. Consistent removal was observed upon exposure to PEG and after 6 h exposure, the total PCBs in mussel was 109.04 ppb. In this batch of sample, PCB 138 and 153 was not detected.

The similar pattern of removal was presumed for in situ treatment with the use of same batch and size of mussels. Nevertheless, in the presence of immobilized photocatalyst, the amount of PCBs identified during the reactions showed vast distinct pattern as displayed in Fig. 9. Large quantity of PCB 28 with PCB 52 was identified after 1 h of degradation which further reduced in the subsequent hour. However, higher amount of PCB 28 and PCB 52 detected after 3 h of reaction suggests the occurrence of simultaneous removal process. The decrease in PCBs amount in the subsequent hours indicates that most of the PCB 28 was degraded to lower chlorinated biphenyls with slower degradation of PCB 52 due to its structure as been reported by Miao et al. [59]. As this batch of mussel sample is similar to control run, PCB 138 and 153 was not detected neither in aqueous nor mussels. This could be due to selectivity of PCB removal that suggests for future study using mixture of different type PEG. Nevertheless, the total PCBs detected in the mussels after the reaction (14.97 ppb) showed remarkable difference compared to the control test. Consequently, by comparing the results obtained from

Figs. 8 and 9, it is expected that in the presence of photocatalyst and light irradiation, the removed PCBs were degraded instantly which demonstrated the efficiency of the method.

3.5. Proposed reaction mechanism

The proposed mechanism involves two steps which is the removal of PCBs from mussel using PEG and followed by photodegradation as shown in Scheme 1. The reaction studied is a typical nucleophilic substitution with PEG behaves as a potent nucleophilic agent. Due to its high lipophilicity, PEG also acts as phase transfer catalyst, moving polychlorobiphenyl molecules from the apolar phase (lipid) to the polar phase ($\text{PEG}/\text{H}_2\text{O}$) involving electrostatic interaction and hydrogen bonding forming aryl polyethylene glycol. The removal reaction however did not attain 100% showing that the interaction between PEG and PCB occurred only at the interface as well as the selectivity factor.

Subsequent reaction in the presence of photocatalyst with high acidity (as shown by $\text{NH}_3\text{-TPD}$) resulted in adsorption of chlorine atom on polychlorinated biphenyl molecule onto the catalyst surface by strong interaction with catalyst bridging OH. A strong correlation between acidity, type of acid sites and interaction between chloroaromatic adsorption on catalyst surface has been described by Albonetti et al. [62]. The increased surface acidity of WST-M photocatalyst enables the adsorption of more hydroxyl group in addition to more organic reactants on its surface which obviously facilitate the enhancement of photocatalytic activity.

Upon irradiation with light, the excitation of metal oxides causes the generation of electron-hole pairs and charge transfer between the metal oxides. In a heterojunction structured semiconductor, the photogenerated electron are transferred from the higher to lower conduction band while holes from the higher to lower valence band. According to the Mulliken electronegativity theory [46], the potential energy of conduction band (CB) and valence band (VB) were estimated for TiO_2 ($E_{\text{CB}} = -0.07 \text{ eV}$; $E_{\text{VB}} = 2.99 \text{ eV}$), SnO_2 ($E_{\text{CB}} = -0.01 \text{ eV}$; $E_{\text{VB}} = 3.47 \text{ eV}$) and WO_3 ($E_{\text{CB}} = 0.49 \text{ eV}$; $E_{\text{VB}} = 3.05 \text{ eV}$). Hence, the photoexcited electrons could be transferred from conduction band of TiO_2 to SnO_2 and WO_3 . The charge transfer process between $\text{TiO}_2 \rightarrow \text{SnO}_2 \rightarrow \text{WO}_3$ was also evident from XPS spectra (Fig. S10) [46]. The shifting in binding energy as

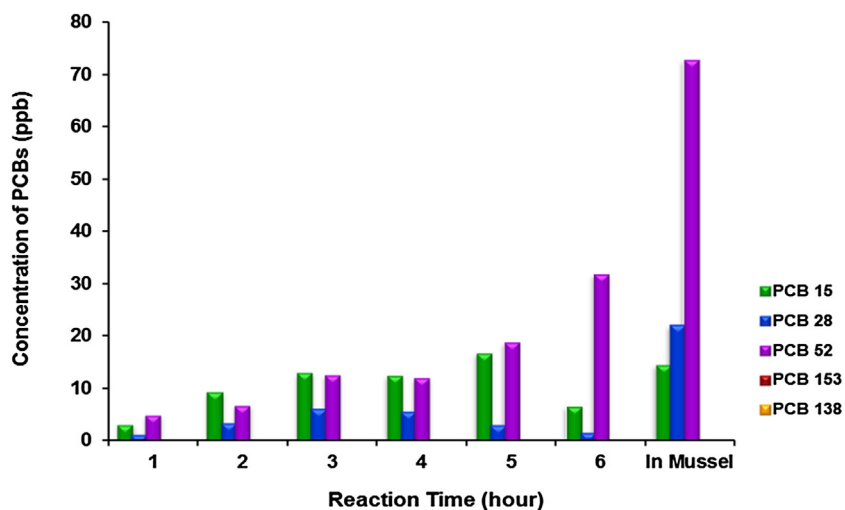


Fig. 8. Concentration of PCBs in aqueous during a control test under visible light for 6 h in the absence of photocatalyst together with the concentration of PCBs in mussels after reaction.

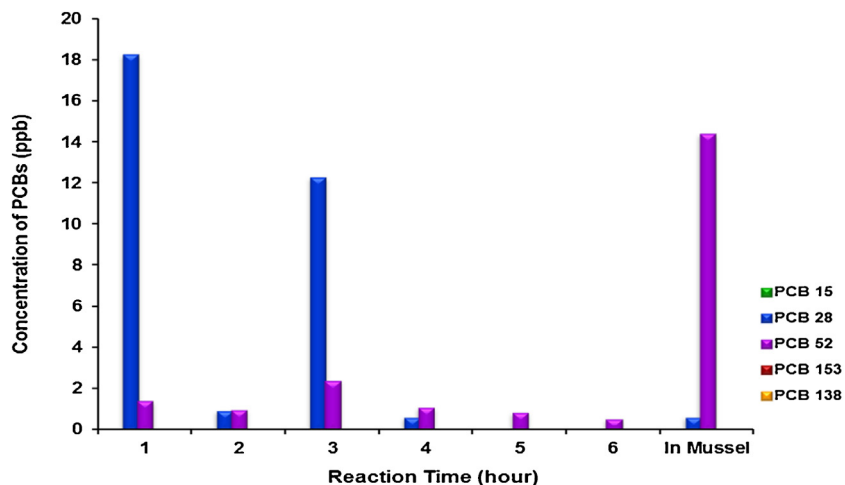
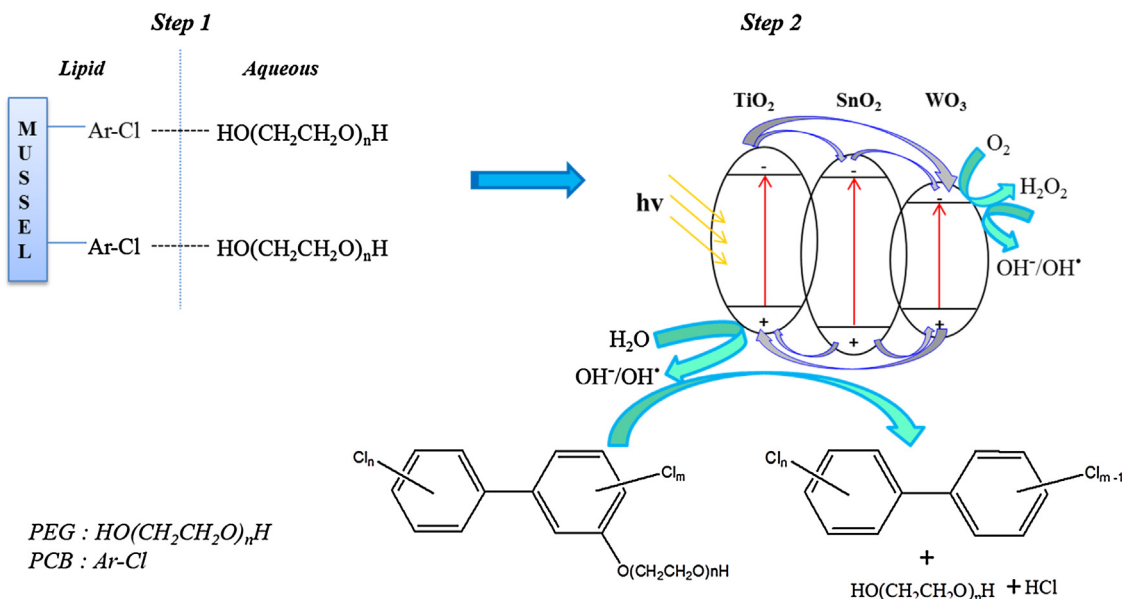


Fig. 9. Concentration of PCBs in aqueous during in situ removal and photocatalytic degradation of PCBs using immobilized photocatalyst under visible light for 6 h together with concentration of PCBs in mussels after complete reaction.



Scheme 1. Proposed mechanism for the removal of PCBs from mussel using PEG followed by photocatalytic degradation using immobilized WST-M photocatalyst.

well as the reduced Ti^{3+} and increased W^{5+} in the WST-M compared to pure metal oxides demonstrate the occurrence of charge transfer between the metal oxides as also supported by Li et al. [63] and Xiaodong et al. [64]. Due to the lower conduction band of WO_3 compared to $(E(O_2/\bullet O_2^-) = -0.046\text{ eV vs NHE})$, the accumulated electrons on conduction band of WO_3 reacts with O_2 forming H_2O_2 ($E(O_2/H_2O_2) = +0.70\text{ eV vs NHE}$) which are further reduced to OH^\bullet and OH^- . On the other hand, holes in valence band of TiO_2 which is more positive than the standard redox potential of OH^-/OH^\bullet (1.99 eV vs. NHE) have strong oxidizing power to oxidize OH^- or H_2O to OH^\bullet [65]. The effect of scavengers such as *tert*-butanol (OH^\bullet), triethanolamine (h^+), and 1,4-benzoquinone ($\bullet O_2^-$) on photodegradation of 1,2-dichlorobenzene as model PCB has been evaluated in earlier study. As shown in Fig. S11, the reaction has been mostly inhibited by the presence of OH^\bullet but showed negative result with the addition of 1,4-benzoquinone. This reveals that the photocatalytic process is mainly governed by OH^\bullet and h^+ rather than $\bullet O_2^-$ which is in line with the proposed radical formation based on the redox potential energy. Accordingly, it could be concluded that with the presence of OH^-/OH^\bullet , the adsorbed PCB finally undergoes dechlorination via electrophilic substitution.

Since PEG combined with PCB after the removal stage formed arylpolyglycol and the ease of C–Cl bond breaking is higher than C–O, the decomposition of PEG was not observed in this experiment. Besides, previous study has reported enhanced reductive dechlorination of PCB in the presence of alcohol and photoexcited TiO_2 [66]. The dechlorination occurred by electron transfer from ketyl radical anion formed by hydroxyl ion attack during the photocatalytic activity. Accordingly, prolonged photocatalytic reaction with the existence of hydroxyl ion would result in bond breaking of the aromatic ring. Therefore, this method can be considered as a convenient and economical way for its low cost and sustainability in PCBs removal from sea catches as mussels.

4. Conclusion

This study reported a novel successive process for the removal of PCBs from mussels using phase transfer agent followed by photocatalysis technique for its degradation in aqueous. A significant portion of total PCBs could be removed from the mussels by using appropriate type and concentration of PEG, in this case PEG 400 (0.2 M). The removed PCBs in aqueous medium could be further degraded under visible light with the presence of mechanical mixed $WO_3/SnO_2/TiO_2$ photocatalyst. In situ and ex situ treatment techniques were evaluated whereby both methods exhibited reduced PCBs level in mussels. The results obtained suggest that the majority of PCBs were dechlorinated during the photocatalytic reaction. Thus, this approach can be considered a safe and cost-effective remediation technology. For future improvement, study on mixture of different types of PEG to enhance selectivity of PCBs as well as choice of food grade metal oxides are essential in order to make this method reliable option for remediation activities.

Acknowledgements

This work was financially supported by Universiti Teknologi Malaysia for project titled 'Application of Titania Based Trimetallic Oxide Catalyst For Degradation of 1,2-Dichlorobenzene and Polychlorinated Biphenyl in Aqueous' under the Post-Doctoral Fellowship Scheme.

Appendix A. Supplementary data

Supplementary data associated with this article can be found, in the online version, at <http://dx.doi.org/10.1016/j.apcatb.2017.06.066>.

References

- [1] Y. Xing, Y. Lu, R.W. Dawson, Y. Shi, H. Zhang, T. Wang, W. Liu, W. Ren, A spatial temporal assessment of pollution from PCBs in China, *Chemosphere* 60 (2005) 731–739.
- [2] Y.X. Sun, Q. Hao, X.R. Xu, X.J. Luo, S.L. Wang, Z.W. Zhang, B.X. Mai, Persistent organic pollutants in marine fish from Yongxing Island, South China Sea: levels, composition profiles and human dietary exposure assessment, *Chemosphere* 98 (2014) 84–90.
- [3] D. Ueno, T. Isobe, K. Ramu, S. Tanabe, M. Alaee, C. Marvin, K. Inoue, T. Someya, T. Miyajima, H. Kodama, H. Nakata, Spatial distribution of hexabromocyclododecanes (HBCDs), polybrominated diphenyl ethers (PBDEs) and organochlorines in bivalves from Japanese coastal waters, *Chemosphere* 78 (2010) 1213–1219.
- [4] G. Devanathan, A. Subramanian, A. Sudaryanto, S. Takahashi, T. Isobe, S. Tanabe, Brominated flame retardants and polychlorinated biphenyls in human breast milk from several locations in India: potential contaminant sources in a municipal dumping site, *Environ. Int.* 39 (2012) 87–95.
- [5] P. Montuori, T. Cirillo, E. Fasano, A. Nardone, F. Esposito, M. Triassi, Spatial distribution and partitioning of polychlorinated biphenyl and organochlorine pesticide in water and sediment from Sarno River and Estuary, Southern Italy, *Environ. Sci. Pollut. Res.* 21 (2014) 5023–5035.
- [6] R. Yang, Y. Wang, A. Li, Q. Zhang, C. Jing, T. Wang, P. Wang, Y. Li, G. Jiang, Organochlorine pesticides and PCBs in fish from lakes of the Tibetan Plateau and the implications, *Environ. Pollut.* 158 (2010) 2310–2316.
- [7] A. Aksoy, Y.K. Das, O. Yavuz, D. Guvenc, E. Atmaca, S. Agaoglu, Organochlorine pesticide and polychlorinated biphenyls levels in fish and mussel in Van Region Turkey, *Bull. Environ. Contam. Toxicol.* 87 (2011) 65–69.
- [8] D. Kožul, S.H. Romanic, Z. Kljaković-Gaspic, J. Veza, Distribution of polychlorinated biphenyls and organochlorine pesticides in wild mussels from two different sites in central Croatian Adriatic coast, *Environ. Monit. Assess.* 179 (2011) 325–333.
- [9] I. Cok, B. Mazmancı, M.A. Mazmancı, C. Turgut, B. Henkelmann, K.W. Schramm, Analysis of human milk to assess exposure to PAHs PCBs and organochlorine pesticides in the vicinity Mediterranean city Mersin, Turkey, *Environ. Int.* 40 (2012) 63–69.
- [10] G.O. Thomas, M. Wilkinson, S. Hodson, K.C. Jones, Organohalogen chemicals in human blood from the United Kingdom, *Environ. Pollut.* 141 (2006) 30–41.
- [11] M.N. Ahmed, S.N. Sinha, S.R. Vemula, P. Sivaperumal, K. Vasudev, S. Ashu, V.R.M. Vishnu, V. Bhatnagar, Accumulation of polychlorinated biphenyls in fish and assessment of dietary exposure: a study in Hyderabad City, India, *Environ. Monit. Assess.* 188 (2016) 94.
- [12] S. Bayen, G.O. Thomas, H.K. Lee, J.P. Obbard, Occurrence of polychlorinated biphenyls and polybrominated diphenyl ethers in green mussels (*Perna Viridis*) from Singapore, Southeast Asia, *Environ. Toxicol. Chem.* 22 (2003) 2432–2437.
- [13] R. Matsumoto, N.P.C. Tu, S. Haruta, M. Kawano, I. Takeuchi, Polychlorinated biphenyl (PCB) concentrations and congener composition in masu salmon from Japan: a study of all 209 PCB congeners by high-resolution gas chromatography/high-resolution mass spectrometry (HRGC/HRMS), *Mar. Pollut. Bull.* 85 (2014) 549–557.
- [14] U.H. Yim, S.H. Hong, W.J. Shim, J.R. Oh, Levels of persistent organochlorine contaminants in fish from Korea and their potential health risk, *Arch. Environ. Contam. Toxicol.* 48 (2005) 358–366.
- [15] K. Ramu, N. Kajiwara, T. Isobe, S. Takahashi, E. Kim, B. Min, S. We, S. Tanabe, Spatial distribution and accumulation of brominated flame retardants, polychlorinated biphenyls and organochlorine pesticides in blue mussels (*Mytilus edulis*) from coastal waters of Korea, *Environ. Pollut.* 148 (2007) 562–569.
- [16] B.K. Greenfield, R.M. Allen, Polychlorinated biphenyl spatial patterns in San Francisco Bay forage fish, *Chemosphere* 90 (2013) 1693–1703.
- [17] B. Subedi, S. Yun, S. Jayaraman, B.J. Bergen, K. Kannan, Retrospective monitoring of persistent organic pollutants, including PCBs, PBDEs, and polycyclic musks in blue mussels (*Mytilus edulis*) and sediments from New Bedford Harbor, Massachusetts, USA: 1991–2005, *Environ. Monit. Assess.* 186 (2014) 5273–5284.
- [18] R. Bettinetti, S. Quadroni, E. Boggio, S. Galassi, Recent DDT and PCB contamination in the sediment and biota of the Como Bay (Lake Como, Italy), *Sci. Total Environ.* 542 (2016) 404–410.
- [19] I. Blanchet-Letrouve, A. Zalouk-Vergnoux, A. Venisseau, M. Couderc, B.L. Bizec, P. Elie, C. Herrenknecht, C. Mouneyrac, L. Poirier, Dioxin-like, non-dioxin like PCB and PCDD/F contamination in European eel (*Anguilla anguilla*) from the Loire estuarine continuum: spatial and biological variabilities, *Sci. Total Environ.* 472 (2014) 562–571.
- [20] D. Costopoulou, I. Vassiliadou, L. Leondiadis, PCDDs, PCDFs and PCBs in farmed fish produced in Greece: levels and human population exposure assessment, *Chemosphere* 146 (2016) 511–518.
- [21] R. Malisch, A. Kotz, Dioxins and PCBs in feed and food – review from European perspective, *Sci. Total Environ.* 491/492 (2014) 2–10.
- [22] EU/711/2013, Commission Recommendation 2013/711/EU of 3 December 2013 on the reduction of the presence of dioxins, furans and PCBs in feed and food as amended by Commission Recommendation 2014/663/EU of 11 September 2014, <https://www.epa.gov/dwstandardsregulations>, 2016 (Accessed 2 April 2016).

[23] P. Larsson, Contaminated sediments of lakes and oceans act as sources of chlorinated hydrocarbons for release to water and atmosphere, *Nature* 317 (1985) 347–349.

[24] K. Ayato, I. Ryouji, H. Katsuhisa, Experimental study on the removal of dioxins and coplanar polychlorinated biphenyls (PCBs) from fish oil, *J. Agric. Food Chem.* 54 (2006) 10294–10299.

[25] B. Barbara, G. Upal, Field-scale reduction of PCB bioavailability with activated carbon amendment to river sediments, *Environ. Sci. Technol.* 45 (2011) 10567–10574.

[26] Y.M. Cho, U. Ghosh, A.J. Kennedy, A. Grossman, G. Ray, J.E. Tomaszewski, D.W. Smithery, T.S. Bridges, R.G. Luthy, Field application of activated carbon amendment for in-situ stabilization of polychlorinated biphenyls in marine sediment, *Environ. Sci. Technol.* 43 (2009) 3815–3823.

[27] B. Pamela McLeod, J.V.H. Martine, N.L. Samuel, G.L. Richard, Biological uptake of polychlorinated biphenyls by *Macoma balthica* from sediment amended with activated carbon, *Environ. Toxicol. Chem.* 26 (2007) 980–987.

[28] H. Fadaei, A. Watson, A. Place, J. Connolly, U. Ghosh, Effect of PCB bioavailability changes in sediments on bioaccumulation in fish, *Environ. Sci. Technol.* 49 (2015) 12405–12413.

[29] D. Kupriyanchyk, M.I. Rakowska, I. Roessink, E.P. Reichman, J.T.C. Grotenhuis, A.A. Koelmans, In situ treatment with activated carbon reduces bioaccumulation in aquatic food chains, *Environ. Sci. Technol.* 47 (2013) 4563–4571.

[30] L.W. Perelo, Review: in situ and bioremediation of organic pollutants in aquatic sediments, *J. Hazard. Mater.* 117 (2010) 81–89.

[31] B. Hosseinkhani, A. Nuzzo, G. Zanaroli, F. Fava, N. Boon, Assessment of catalytic dechlorination activity of suspended and immobilized bio-Pd NPs in different marine conditions, *Appl. Catal. B: Environ.* 168/169 (2015) 62–67.

[32] A. Mercier, C. Joulian, C. Michel, P. Auger, S. Coulon, L. Amalric, C. Morlay, F. Battaglia-Brunet, Evaluation of three activated carbons for combined adsorption and biodegradation of PCBs in aquatic sediment, *Water Res.* 51 (2014) 304–315.

[33] J.L. Domingo, Nutrients and chemical pollutants in fish and shellfish. Balancing health benefits and risks of regular fish consumption, *Crit. Rev. Food Sci. Nutr.* 56 (2016) 979–988.

[34] I.W. Azelee, R. Ismail, R. Ali, W.A.W.A. Bakar, Chelation technique for the removal of heavy metals (As, Pb Cd and Ni) from green mussel, *Perna viridis*, *Indian J. Geo-Mar. Sci.* 43 (2014) 372–376.

[35] C. Lee, R. Doong, Enhanced dechlorination of tetrachloroethylene by zerovalent silicon in the presence of polyethylene glycol under anoxic conditions, *Environ. Sci. Technol.* 45 (2011) 2301–2307.

[36] J.P. Louis, J.T. Edward, Method for the solvent extraction of polychlorinated biphenyls, United States Patent 4,430,208, 1984.

[37] P.D. Filippis, M. Scarsella, F. Pochetti, Dechlorination of polychlorinated biphenyls: a kinetic study of removal of PCBs from mineral oils, *Ind. Eng. Chem. Res.* 38 (1999) 380–384.

[38] S.R. Keon, S.H. Byun, J.H. Choi, Y.P. Hong, Y.T. Ryu, J.S. Song, D.S. Lee, H.S. Lee, Destruction and removal of PCBs in waste transformer oil by a chemical dechlorination process, *Bull. Korean Chem. Soc.* 28 (2007) 520–528.

[39] M. Zorrilla, P. Velazco, G. Villanueva, L.E. Arteaga, H.V. Langenhove, Deshalogenation of Sotol-10 using a no-destructive method: pilot plant design, *Procedia Eng.* 42 (2012) 346–357.

[40] L. Chun-chi, D. Ruey-an, Enhanced dechlorination of tetrachloroethylene by zerovalent silicon in the presence of polyethylene glycol under anoxic conditions, *Environ. Sci. Technol.* 45 (2011) 2301–2307.

[41] G. Liu, J.C. Yu, G.Q. Lu, H.M. Cheng, Crystal facet engineering of semiconductor photocatalysts: motivations, advances and unique properties, *Chem. Commun.* 47 (2011) 6763–6783.

[42] R. Sasikala, A. Shirole, V. Sudarsan, T. Sakuntala, C. Sudakar, R. Naik, S.R. Bharadwaj, Highly dispersed phase of SnO₂ on TiO₂ nanoparticles synthesized by polyol-mediated route: photocatalytic activity for hydrogen generation, *Int. J. Hydrogen Energy* 34 (2009) 3621–3630.

[43] S. Anandan, T. Sivasankar, T.L. Villarreal, Synthesis of TiO₂/WO₃ nanoparticles via sonochemical approach for the photocatalytic degradation of methylene blue under visible light illumination, *Ultrason. Sonochem.* 21 (2014) 1964–1968.

[44] E. Grabowska, J.W. Sobczak, M. Gazda, A. Zaleska, Surface properties and visible light activity of W-TiO₂ photocatalysts prepared by surface impregnation and sol-gel method, *Appl. Catal. B Environ.* 117–118 (2011) 351–359.

[45] R. Nadarajan, W.A.W.A. Bakar, R. Ali, R. Ismail, Photocatalytic degradation of 1,2-dichlorobenzene using immobilized TiO₂/SnO₂/WO₃ photocatalyst under visible light: application of response surface methodology, *Arabian J. Chem.* (2016), <http://dx.doi.org/10.1016/j.arabjc.2016.03.006>, in press.

[46] R. Nadarajan, W.A.W.A. Bakar, R. Ali, R. Ismail, Effect of structural defects towards the performance of TiO₂/SnO₂/WO₃ photocatalyst in the degradation of 1,2-dichlorobenzene, *J. Taiwan Inst. Chem. Eng.* 64 (2016) 106–115.

[47] C. Wang, X. Zhang, B. Yuan, Y. Wang, P. Sun, D. Wang, Multi-heterojunction photocatalysts based on WO₃ nanorods: Structural design and optimization for enhanced photocatalytic activity under visible light, *Chem. Eng. J.* 237 (2014) 29–37.

[48] D. Zhang, L. Zhang, L. Shi, C. Fang, H. Li, R. Gao, L. Huang, J. Zhang, In situ supported MnO_x–CeO_x on carbon nanotubes for the low-temperature selective catalytic reduction of NO with NH₃, *Nanoscale* 5 (2013) 1127–1136.

[49] Y. Shen, S. Zhu, Deactivation mechanism of potassium additives on Ti_{0.8}Zr_{0.2}Ce_{0.2}O_{2.4} for NH₃-SCR of NO, *Catal. Sci. Technol.* 2 (2012) 1806–1810.

[50] R. Jin, Y. Liu, Z. Wu, H. Wang, T. Gu, Low-temperature selective catalytic reduction of NO with NH₃ over Mn-Ce oxides supported on TiO₂ and Al₂O₃: a comparative study, *Chemosphere* 78 (2010) 1160–1166.

[51] K. Suttiponparnit, J. Jiang, M. Sahu, S. Suvachittanont, T. Charinpanitkul, P. Biswas, Role of surface area primary particle size, and crystal phase on titanium dioxide nanoparticle dispersion properties, *Nanoscale Res. Lett.* 6 (2011) 2–8.

[52] K. Nakajoh, T. Muramatsu, Y. Maezawa, M. Kon, T. Todoroki, K. Nishizawa, A. Ohara, Method of treating fats and oils, United States Patent Application Publication, US 2003/0175401 A1, 2003.

[53] C. Antonetti, D. Licursi, A.M.R. Galletti, M. Martinelli, F. Tellini, G. Valentini, F. Gambineri, Application of microwave irradiation for the removal of polychlorinated biphenyls from siloxane transformer and hydrocarbon engine oils, *Chemosphere* 159 (2016) 72–79.

[54] D.J. Brunelle, D.A. Singleton, Destruction/removal of polychlorinated biphenyls from non-polar media: reaction of PCB with poly(ethylene glycol)/KOH, *Chemosphere* 12 (1983) 183–196.

[55] Y. Xiao, J.G. Jiang, H. Huang, Chemical dechlorination of hexachlorobenzene with polyethylene glycol and hydroxide: dominant effect of temperature and ionic potential, *Sci. Rep.* 4 (2014) 1–6.

[56] P.N. Anderson, R.A. Hites, OH radical reactions: the major removal pathway for polychlorinated biphenyls from the atmosphere, *Environ. Sci. Technol.* 30 (1996) 1756–1763.

[57] M.D. Mullins, C.M. Pochini, S. McCrindle, M. Romkes, S.H. Safe, L.M. Safe, High-resolution PCB analysis: synthesis and chromatographic properties of all 209 PCB congeners, *Environ. Sci. Technol.* 18 (1984) 468–476.

[58] Y.J. Lin, Y.L. Chen, C.Y. Huang, W.F. Wu, Photocatalysis of 2,2',3,4,4',5'-hexachlorobiphenyl and its intermediates using various catalytical preparing methods, *J. Hazard. Mater.* 136 (2006) 902–910.

[59] X.S. Miao, S.G. Chu, X.B. Xu, Degradation pathways of PCBs upon UV irradiation in hexane, *Chemosphere* 39 (1999) 1639–1650.

[60] E.D. Felip, F. Ferri, C. Lupi, N.M. Trieff, F. Volpi, A.D. Domenico, Structure-dependent photocatalytic degradation polychlorobiphenyls in a TiO₂ aqueous system, *Chemosphere* 33 (1996) 2263–2271.

[61] Y. Noma, Y. Mitsuhasha, M. Matsuyama, S. Sakai, Pathways and products of the degradation of PCBs by the sodium dispersion method, *Chemosphere* 68 (2007) 871–879.

[62] S. Albonetti, S. Blasioli, R. Bonelli, J.E. Mengou, S. Scire, F. Trifiro, The role of acidity in the decomposition of 1,2-dichlorobenzene over TiO₂-based V₂O₅/WO₃ catalysts, *Appl. Catal. A Gen.* 34 (2008) 18–25.

[63] J. Li, H.C. Zeng, Hollowing Sn-doped TiO₂ nanospheres via oswald ripening, *J. Am. Chem. Soc.* 129 (2007) 15839–15847.

[64] W. Xiaodong, Y. Haining, W. Duan, L. Shuang, J. Fan, Synergistic effect between MnO and CeO₂ in the physical mixture: electronic interaction and NO oxidation activity, *J. Rare Earth* 31 (2013) 1141–1147.

[65] H. Li, Q. Deng, J. Liu, W. Hou, N. Du, R. Zhang, X. Tao, Synthesis, characterization and enhanced visible light photocatalytic activity of Bi₂MoO₆/Zn-Al layered double hydroxide hierarchical heterostructures, *Catal. Sci. Technol.* 4 (2014) 1028–1037.

[66] J.P. Ghosh, G. Achari, C.H. Langford, Reductive dechlorination of PCBs using photocatalyzed UV light, *Clean – Soil Air Water* 40 (2012) 455–460.